# Forward Jetting Phenomenon in Detonations

Patrick A. Meagher[1,*], Xian Shi[2], Jackson Crane[2,#],
Xinyu Zhao[1], Alexei Y. Poludnenko[1], Hai Wang[2]

[1]Department of Mechanical Engineering, University of Connecticut, Storrs, CT, USA
[2]Department of Mechanical Engineering, Stanford University, Stanford, CA, USA

## 1 Introduction

Recently, efforts have been made in understanding the role of the forward jetting phenomenon in Mach stem bifurcation during the early phase of detonation cell formation [1–3]. Mach and Radulescu first extended the analysis of this hydrodynamic phenomenon in inert shocks [2, 4] to detonations, showing that for sufficiently strong forward jetting, the Mach stem is deformed to the point of bifurcating to produce a new triple point [1]. Subsequent studies have shown that jetting, its detailed structure, and its ability to interact with detonation cells are a strong function of mixtures properties, including both chemical kinetics, e.g., global activation energy, $\varepsilon_I$, and hydrodynamics, e.g., ratio of specific heats, $\gamma$ [1, 3]. These studies, however, exploited idealized physical models that cannot be directly compared to experimental results.

The present study aims to study the jetting phenomenon and its dependence on mixture properties through detailed simulations of realistic mixtures. Specifically, by extending previous work on trace ozone addition [5], we discuss the approach for creating experimentally viable mixtures where $\varepsilon_I$ can be controlled independently of other mixture parameters, notably $\gamma$. Two hydrogen-oxygen mixtures with equivalent $\varepsilon_I$ are designed using carbon dioxide (case 1) and argon dilution (case 2), with low and high $\gamma$ values, respectively. Second, we present numerical soot foils from two-dimensional (2D) Navier-Stokes simulations of detonations for the above two cases with the goal to explore the impact of $\gamma$ on the observed cellular structures. The current study considers the effects of detailed thermodynamics, and detailed, finite rate chemistry, and molecular transport, and uses sufficiently wide domains to avoid mode-locked single-headed propagation. Finally, we provide instantaneous snapshots of the typical jet structure for the two mixtures, with an emphasis on the local fluid velocity relative to the instantaneous Mach stem speed.

## 2 Numerical Methods

Compressible Navier-Stokes equations were solved on the fixed uniform grid with a massively parallel code `Athena-RFX` [6, 7], a reactive-flow extension of the magnetohydrodynamics code `Athena` [8]. Convective fluxes were calculated with the HLLC-ADC (Anti-Diffusion Control) scheme to minimize carbuncle phenomenon [9], and flow integration was performed with a second-order accurate Godunov

* **Correspondence to: patrick.meagher@uconn.edu**
# Current address: Department of Chemical Engineering, Queen's University, Kingston, Ontario, Canada

scheme employing the unsplit corner transport upwind (CTU) method [10]. A piecewise linear method (PLM) [11] was used for state reconstruction. Net diffusive fluxes are calculated with a second-order finite difference method with flux matching to maintain conservation [6]. Flow and chemistry were coupled through Strang splitting [12] with a global reaction-advection time-step control. This methodology is second-order in both time and space.

Chemical source terms were integrated using the non-iterative, single-step, semi-implicit ODE integrator YASS [13]. A 12-species chemical kinetic model extracted from FFCM-1 [14] was used for hydrogen combustion with argon, carbon dioxide, and ozone addition. Notably, the submodel includes five reactions of CO and $CO_2$ to account for carbon dioxide dissociation under detonation conditions. Constant volume ignition delay times for detonation-relevant conditions were calculated with both the full model and the submodel used in this study, and good agreement was observed between the two models .

## 3 Computational Configuration

Two 2D simulations were conducted in the laboratory frame of reference, with cellular detonations propagating into a quiescent mixture at 300 K and 40 kPa. Table 1 provides details for the two selected cases, where $x$ and $y$ denote the streamwise and spanwise directions, respectively. All ZND calculations were performed using the Shock and Detonation Toolbox [15]. In both simulations the detonation is resolved with 50 computational cells per induction length $\Delta_i$. The normalized domain width $L_y/\Delta_i$ is fixed at 110 to be sufficiently large to accommodate multiple detonation cells across the domain width while remaining comparable across mixtures. The domain length $L_x$ is sufficiently long to avoid interference from the rear boundary condition for the duration of the simulation. Both simulations were allowed to propagate for $2000\Delta_i$, or 0.132 ms and 0.178 ms for cases 1 and 2, respectively.

Table 1: Details of mixtures for cases 1 and 2. In both cases, the pre-shock temperature $T_0 = 300$ K and pressure $p_0 = 40$ kPa.

| Parameter | Case 1 | Case 2 |
|---|---|---|
| Mixture | $2H_2$-$O_2$-$CO_2$-9000 PPM $O_3$ | $2H_2$-$O_2$-3.76Ar |
| CJ velocity, $D_{\mathrm{CJ}}$ (m/s) | 1980 | 1825 |
| Induction length,[a] $\Delta_i$ ($\mu$m) | 130.1 | 156.3 |
| Exothermic pulse width,[b] $\Delta_e$ ($\mu$m) | 81.49 | 101.9 |
| Physical domain size, $L_x \times L_y$ (mm) | 43.7×14.3 | 81.1×17.2 |
| Normalized domain size, $L_x/\Delta_i \times L_y/\Delta_i$ | 336×110 | 519×110 |
| Grid size, $n_x \times n_y$ | 16800×5504 | 25952×5504 |
| Ratio of specific heats,[c] $\gamma_{VN}$ | 1.267 | 1.439 |
| Global activation energy [16], $\varepsilon_I$ | 4.700 | 4.682 |

[a] Induction length $\Delta_i$ defined as the distance from shock to peak thermicity in the ZND solution.
[b] Exothermic pulse width $\Delta_e$ defined as the full width at half maximum of thermicity (FWHM).
[c] Ratio of specific heats calculated at the von Neumann state.

In both cases, the upstream boundary condition is zero-gradient and downstream boundary is fixed at the CJ state. All transverse walls have adiabatic, slip boundary conditions. Detonations were initialized with a spatially perturbed sinusoidal ZND profile. This approach rapidly produces transverse waves and minimizes the initial transient period. To minimize the computational cost, a moving grid technique is employed, which removes the burnt region and introduces fresh quiescent gas upstream at discrete intervals.

## 4 Results and Discussion

### 4.1 Mixture Design Through Ozone Addition

Through addition of trace amounts of ozone, $\varepsilon_I$ for a given mixture can be reduced without producing appreciable changes in the mixture's thermodynamic properties, CJ states, and detonation speed [5]. For this study, $\varepsilon_I$ was estimated from the constant volume ignition delay calculations, as outlined in Ref. [16]. The mixture design procedure is to identify first a target low-$\varepsilon_I$ / high-$\gamma$ composition. The widely-studied hydrogen-oxygen-argon mixture is selected and denoted as case 2. Then a mixture with low $\gamma$ is selected with the only constraint that $\varepsilon_I$ is the same as that of the argon-diluted mixture, possibly achieved through ozone doping. For this case, fuel/oxidizer was maintained as a stoichometric mixture of hydrogen and oxygen, and carbon dioxide was chosen as the diluent. Carbon dioxide is a favorable low-$\gamma$ diluent both numerically and experimentally, being readily available and with well established thermochemical properties. The global activiation energy $\varepsilon_I$ was then calculated for increasing amounts of ozone addition until a $\varepsilon_I$ close to that of case 2 was achieved. Under the conditions studied, 9000 PPM of ozone was found to be sufficient to reduce $\varepsilon_I$ of the carbon dioxide diluted mixture (case 1) to that of the argon diluted mixture (case 2).

### 4.2 Effect of $\gamma$ on Cellular Structure

To evaluate the role of $\gamma$ on the detonation structure, Fig. 1 shows pressure-based numerical soot foils for the two simulation cases in normalized spatial coordinates. Both soot foils were extracted after $1000\Delta_i$ of the propagation distance, where the results are independent of the initial conditions. While the cell structures of both mixtures are fairly regular, in case 1 we do observe four clear shock bifurcations generating new triple points, notated by the red arrows. At both $x/\Delta_i \approx 1000$ and $x/\Delta_i \approx 2000$ there are five detonation cells across the domain width, indicating that these particular shock bifurcations are accompanied by the destruction of the original triple points. This behavior is entirely absent in case 2, where no shock bifurcation or triple point destruction is observed. Decreasing $\gamma$ is also quantitatively shown to produce a more irregular detonation structure, with the standard deviation of cell length $\ell$, width $\lambda$, and aspect ratio $\ell/\lambda$ for case 1 being 10%, 13%, and 8%, respectively, compared to 9%, 9%, and 4% for case 2. From both qualitative and quantitative evaluation of the soot foils, we conclude that for mixtures of the specific $\varepsilon_I$ value studied here, increasing $\gamma$ is sufficient to regulate detonation cellular structures, while decreasing $\gamma$ can induce shock bifurcations, consistent with previous findings using idealized physical models [3].

### 4.3 Effect of $\gamma$ on the Forward Jets

Figure 2 provides snapshots of the typical jet structures for both the low and high $\gamma$ mixtures, with the detonation propagating from left to right. The local laboratory frame velocity magnitude $|\vec{V}|$ is normalized by the instantaneous Mach stem propagation speed $D$. A black contour is drawn at $|\vec{V}|/D = 1$, and demarcates regions of fluid locally approaching and falling behind the Mach stem. The laboratory frame velocity vector is generally well aligned with the positive $x$ direction (horizontally to the right in Fig. 2), so large $|\vec{V}|$ indicates fast flow in the upstream direction. For case 1, deformation of the Mach stem by the typical strong jet is observed, generating "kinks" on the Mach stem surface above and below the jet. Somewhat unexpectedly, case 2, where these bifurcations do not occur, still contains a significant volume of fluid that propagates upstream in excess of the local Mach stem speed. While the jet in case 1 contains a significantly larger fluid volume and is moving faster compared to the Mach stem than case

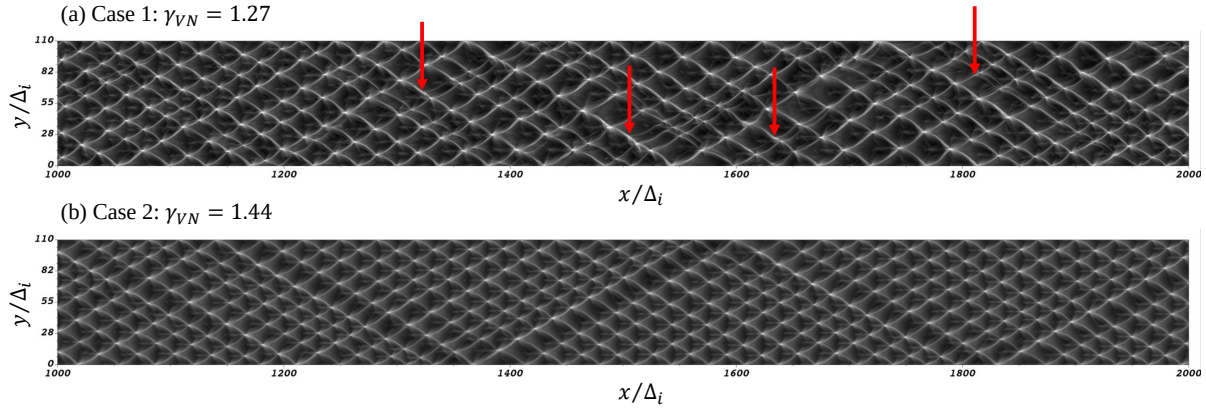


Figure 1: Maximum-pressure-based numeric soot foils for case 1 (low $\gamma$) and case 2 (high $\gamma$). Detonation propagates from left to right. Spatial coordinates are all normalized by induction length $\Delta_i$. Red arrows denote locations of shock bifurcations due to strong forward jets.

2, the jet in case 2 persists until the midpoint of the cell cycle $t_2$, where the center of the jet has finally decayed to $|\vec{V}|/D \approx 1$.

Two additional observations can be made from Fig. 2. First, in both cases the jets are noticeably misaligned with the streamwise direction, slightly downward for case 1 and upward in case 2. This misalignment can be captured only in simulations where multiple cells span the domain width, as reflective boundaries will impose a symmetry condition at the walls forcing streamwise alignments. Second, the angle of the incident shock near the triple point, denoted as $\theta_1$ and $\theta_2$ for case 1 and 2, respectively, is noticeably steeper for case 1 than for case 2. This angle is similar to the ramp angle for inert mixtures, and an increase in ramp angle has been shown to increase the strength of the forward jet [4].

## 5 Concluding Remarks

Three main points are raised through the current investigation. First, we provide a novel framework to design experimentally viable detonable mixtures with a desired $\varepsilon_I$ through trace addition of ozone. Second, using mixtures developed through this approach, we corroborate previous findings that reduction in $\gamma$ alone is sufficient to induce forward jet bifurcations, extending this understanding to realistic mixtures and simulations employing detailed chemical models and molecular transport. Third, we show that the forward jet is present across all mixtures independent of the presence of bifurcation, albeit such a jet is much weaker in high $\gamma$ mixtures.

As a final point, we note that while forward jet-driven bifurcation is most common in low $\gamma$ mixtures, the forward jet is ubiquitous to all mixtures. We propose an unambiguous definition of the forward jet independent of bifurcation as *a region of collimated fluid behind the Mach stem traveling in excess of the instantaneous Mach stem speed*. We hypothesize that these jets act as an energy transfer mechanism and contribute to the local overdrive necessary for cellular detonations to exist. Future work will explore the distribution and impact of jet alignment and incident shock angle on cell regularity, and in particular, it will study forward jets as a mechanism of the overdrive generation.

## Acknowledgements

PAM and XZ acknowledge funding support through the Air Force Office of Scientific Research (AFOSR) under Grant FA9550-18-1-0173. XS, JC, and HW acknowledge funding support through AFOSR under

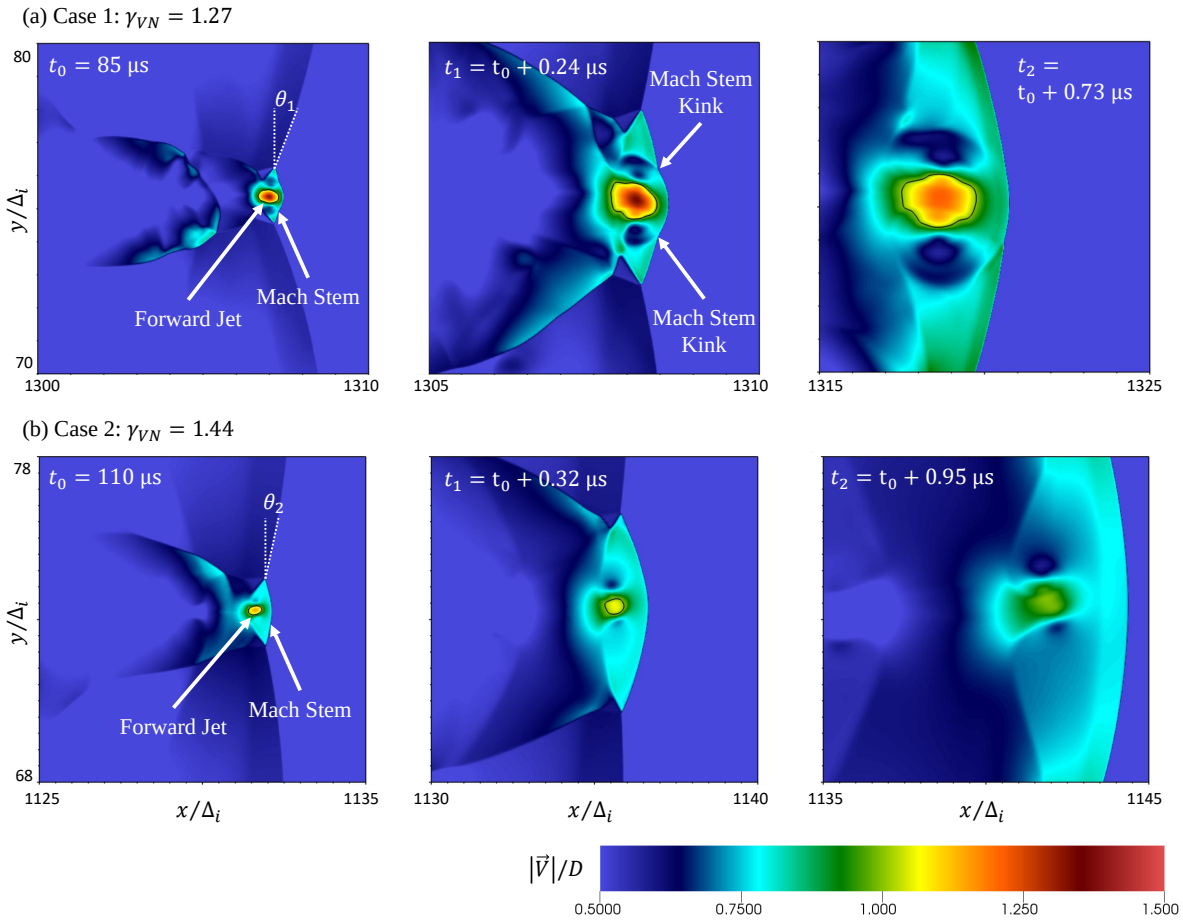


Figure 2: Local fluid velocity magnitude in the laboratory frame normalized by the instantaneous Mach stem speed for (a) case 1 and (b) case 2. A black contour line surrounds fluid where the local velocity magnitude exceeds the Mach stem speed. The detonation is propagating from left to right.

Grant FA9550-20-1-0398. AYP acknowledges funding support through AFOSR under Grant FA9550-21-1-0012 (Program Manager: Dr. Chiping Li). The computational resources are provided in part by the DoD High Performance Computing Modernization Program.

## References

[1] P. Mach and M. Radulescu, "Mach reflection bifurcations as a mechanism of cell multiplication in gaseous detonations," *Proceedings of the Combustion Institute*, vol. 33, pp. 2279–2285, Jan. 2011.

[2] S. S.-M. Lau-Chapdelaine, Q. Xiao, and M. I. Radulescu, "Viscous jetting and Mach stem bifurcation in shock reflections: experiments and simulations," *Journal of Fluid Mechanics*, vol. 908, Dec. 2020.

[3] A. Sow, S.-M. Lau-Chapdelaine, and M. Radulescu, "The effect of the polytropic index $\gamma$ on the structure of gaseous detonations," *Proceedings of the Combustion Institute*, vol. 38, no. 3, pp. 3633–3640, 2021.

[4] L. F. Henderson, E. I. Vasilev, G. Ben-Dor, and T. Elperin, "The wall-jetting effect in mach reflection: theoretical consideration and numerical investigation," *Journal of Fluid Mechanics*, vol. 479, pp. 259–286, Mar. 2003.

[5] J. Crane, X. Shi, A. V. Singh, Y. Tao, and H. Wang, "Isolating the effect of induction length on detonation structure: Hydrogen–oxygen detonation promoted by ozone," *Combustion and Flame*, vol. 200, pp. 44–52, Feb. 2019.

[6] A. Poludnenko and E. Oran, "The interaction of high-speed turbulence with flames: Global properties and internal flame structure," *Combustion and Flame*, vol. 157, no. 5, pp. 995 – 1011, 2010.

[7] Y. Kozak, S. Dammati, L. Bravo, P. Hamlington, and A. Poludnenko, "WENO interpolation for Lagrangian particles in highly compressible flow regimes," *Journal of Computational Physics*, vol. 402, p. 109054, 2020.

[8] J. M. Stone, T. A. Gardiner, P. Teuben, J. F. Hawley, and J. B. Simon, "Athena: A new code for astrophysical MHD," *The Astrophysical Journal Supplement Series*, vol. 178, pp. 137–177, Sept. 2008.

[9] S. Simon and J. Mandal, "A cure for numerical shock instability in HLLC Riemann solver using antidiffusion control," *Computers & Fluids*, vol. 174, pp. 144 – 166, 2018.

[10] T. A. Gardiner and J. M. Stone, "An unsplit Godunov method for ideal MHD via constrained transport in three dimensions," *Journal of Computational Physics*, vol. 227, no. 8, pp. 4123 – 4141, 2008.

[11] E. F. Toro, *Riemann solvers and numerical methods for fluid dynamics: a practical introduction*. Springer Science & Business Media, 2013.

[12] G. Strang, "On the construction and comparison of difference schemes," *SIAM journal on numerical analysis*, vol. 5, no. 3, pp. 506–517, 1968.

[13] A. Khokhlov, "Yass-yet another stiff solver that works," NRL Technical Memorandum Report, 1999.

[14] G. Smith, Y. Tao, and H. Wang, "Foundational Fuel Chemistry Model Version 1.0 (FFCM-1)," 2016.

[15] Shock and Detonation Toolbox - 2021 Version, Explosion Dynamics Laboratory, California Institue of Technology, https://shepherd.caltech.edu/EDL/PublicResources/sdt/, 2021.

[16] H. D. Ng, M. I. Radulescu, A. J. Higgins, N. Nikiforakis, and J. H. S. Lee, "Numerical investigation of the instability for one-dimensional Chapman–Jouguet detonations with chain-branching kinetics," *Combustion Theory and Modelling*, vol. 9, pp. 385–401, Aug. 2005.